Mon. Not. R. Astron. Soc. **000**, 1–?? (2010) Printed February 25, 2014 (MN LATEX style file v2.2)

"Quasi-periodical components in the radial distributions of cosmologically remote objects"

A. I. Ryabinkov[1], A. D. Kaminker[1,2] ⋆
[1] *Ioffe Physical Technical Institute, Politekhnicheskaya 26, 194021 St. Petersburg, Russia,*
[2] *St. Petersburg State Polytechnical University, Politekhnicheskaya 29,*
St. Petersburg, 195251 Russia,
e-mail: calisto@rbcmail.ru, kam@astro.ioffe.ru

arXiv:1402.5597v1 [astro-ph.CO] 23 Feb 2014

Accepted 2011 xxxx. Received 2011 xxxx; in original form 2011 xxxx

ABSTRACT
A statistical analysis of radial (line-of-sight) 1D-distributions of brightest cluster galaxies (BCGs) within the redshift interval $0.044 \leqslant z \leqslant 0.78$ and Mg II absorption-line systems ($0.37 \leqslant z \leqslant 2.28$) is carried out. Power spectra and two-point radial correlation functions are calculated. It is found that both radial distributions of spectroscopic redshifts of 52,683 BCGs and 32,840 Mg II absorption systems incorporate similar quasi-periodical components relatively to the comoving distance. Significance of the components exceeds 4σ-level and admits an increase ($\gtrsim 5\sigma$) for some broad subsamples. For the ΛCDM cosmological model the periodicities correspond to spatial comoving scales (98 ± 3) and (101 ± 2) h^{-1} Mpc, respectively. These quasi-periods turn out to be close to the characteristic scale (101 ± 6) h^{-1} Mpc of the quasi-periodical component obtained earlier for the radial distribution of luminous red galaxies (LRGs). On the other hand, the scales are close to the spatial scale corresponding to the baryon acoustic oscillations (BAOs) revealed by many authors at the last decade. Fourier transform phases obtained for the BCGs and LRGs are found to be close, while the phases calculated for the Mg II absorption systems and LRGs are opposite. Discussions of the results in a context of the BAO and large-scale structure characteristic scales are outlined.

Key words: galaxies: distances and redshifts; quasars: absorption lines; cosmology: observations – distance scale – large-scale structure of Universe

1 INTRODUCTION

We continue a series of works on a research of quasi-periodical scales in radial (line-of-sight) 1D-distributions of various cosmologically remote objects. The first two papers of this series (Ryabinkov, Kaminker & Varshalovich 2007; Ryabinkov & Kaminker 2011, hereafter Papers I and II) investigated quasi-periodical features in the spatial-temporal distribution of 2003 and 2322 absorption-line systems (ALSs) detected in the spectra of 661 and 730 QSOs, respectively, within the cosmological redshift interval $z = 0.0$–4.3. In Paper II we revealed the existence of quasi-periodicity at a scale $\Delta \mathrm{D}_c = (108 \pm 6)\ h^{-1}$ Mpc, where D_c is a line-of-sight comoving distance to an ALS with absorption redshift z_{abs}. It was used the ΛCDM cosmological model with dimensional density parameter $\Omega_\mathrm{m} = 0.23$. The third paper (Ryabinkov, Kaurov & Kaminker 2013, hereafter Paper III) analyzed the radial distribution of 106,000 luminous red galaxies (LRGs) from the Sloan Digital Sky Survey (SDSS) catalogue, data release 7 (DR7), and found two most significant peaks in its power spectrum. The peaks correspond to the spatial comoving scales $(135 \pm 12)\ h^{-1}$ Mpc and $(101\pm6)\ h^{-1}$ Mpc at the ΛCDM model with $\Omega_\mathrm{m} = 0.25$. The latter peak is the dominant with significance $\gtrsim 4\sigma$.

The appropriate scale of quasi-periodicity is in mutual accordance with the period found for the radial distribution of ALSs, especially if one takes into account that at $\Omega_\mathrm{m} = 0.25$ the spatial ALS-scale shifts to $\Delta \mathrm{D}_c = (105 \pm 6)\ h^{-1}$ Mpc. Moreover, both scales are in agreement with a spatial scale $(102.2 \pm 2.8)\ h^{-1}$ Mpc (Blake et al. 2011), which is widely accepted to be the scale of sound horizon, r_s, at the recombination epoch displaying itself in cosmological galactic surveys as the spatial scale corresponding to the baryon acoustic oscillations (BAOs; e.g., Eisenstein & Hu 1998; Eisenstein, Hu & Tegmark 1998; Blake & Glazebrook 2003; Eisenstein et al. 2005; Eisenstein, Seo & White 2007; Bassett & Hlozek 2009; Kazin et al. 2010; Anderson et al. 2012; Ross et al. 2012, and references therein). To confirm

⋆ Send offprint request to: A. D. Kaminker

statistically faintly outlined relations between the BAO-phenomenon (mainly appearing in Fourier space) and the quasi-periodical components of the radial distribution of matter it seems to be reasonable to examine different types of cosmologically remote objects in similar techniques. This is one of the causes motivating us to carry out the present statistical treatment.

In this paper we deal with the radial distributions of two independent sets of cosmological data: (a) the spectroscopic redshifts z of 52,683 so-called brightest cluster galaxies (BCGs) or the most luminous galaxies among constituents of clusters (Wen & Han 2013) within the interval $0.044 \leqslant z \leqslant 0.78$, and (b) the redshifts of 32,840 intervening Mg II ALSs within the interval $0.37 \leqslant z_{abs} \leqslant 2.28$ (Zhu & Ménard 2013). The updated catalog (a) of the BCGs sampled from spectral data of the SDSS DR9 catalog (Ahn et al. 2012) is available on the website [1]; the data (b) are based on the SDSS DR7 catalog (e.g. Abazajian et al. 2009) and represented on the website[2]. To carry out the statistical considerations we calculate the power spectra of radial distributions and separately – two-point radial correlation functions (RCFs).

The basic value of the power spectra calculations is a radial function $\mathrm{N(D}_c\mathrm{)}$ integrated over angles α (right ascension) and δ (declination), $\mathrm{D}_c(z)$ is the line-of-sight comoving distance between an observer and cosmological objects under study; $\mathrm{N(D}_c\mathrm{)dD}_c$ is a number of objects inside an interval dD_c. The radial comoving distances are calculated in a standard way (e.g., Kayser, Helbig & Schramm 1997; Hogg 1999)

$$\mathrm{D}_c(z_i) = \frac{c}{H_0}\int_0^{z_i}\frac{1}{\sqrt{\Omega_m(1+z)^3+\Omega_\Lambda}}\mathrm{d}z, \qquad (1)$$

where i numerates redshifts z_i of cosmological objects in a sample, $H_0 = 100\,h$ km s^{-1} is the present Hubble constant, c is the speed of light, $c/H_0 = 2998\ h^{-1}$ Mpc; it is accepted that the dimensionless density parameters are $\Omega_m = 0.25$ and $\Omega_\Lambda = 1 - \Omega_m = 0.75$. We use the binning approach and calculate so-called normalized radial distribution function:

$$\mathrm{NN(D}_c\mathrm{)} = \frac{\mathrm{N(D}_c\mathrm{)} - \mathrm{N}_{\mathrm{tr}}\mathrm{(D}_c\mathrm{)}}{\sqrt{\mathrm{N}_{\mathrm{tr}}\mathrm{(D}_c\mathrm{)}}}, \qquad (2)$$

where $\mathrm{N}_{\mathrm{tr}}\mathrm{(D}_c\mathrm{)}$ is a smoothed function filtering out the largest scales (trend function). The denominator $\sqrt{\mathrm{N}_{\mathrm{tr}}}$ in Eq. (2) stands for the standard deviation of the Poisson statistics. Examples of the trend function are represented in Fig. 1, where the trends are calculated by the least-squares method with using a set of parabolas, as regression functions for $\mathrm{N(D}_c\mathrm{)}$, and independent bins $\Delta_c = 10\ h^{-1}$ Mpc.

Note that instead of the radial distribution function $\mathrm{N(D}_c\mathrm{)}$ one can use a comoving number density $n(\mathrm{D}_c) = \mathrm{N(D}_c\mathrm{)}/\mathrm{dV}_c$, where $\mathrm{dV}_c{=}4\pi\mathrm{D}_c^2\mathrm{dD}_c$ is a comoving differential volume in the flat Universe, that is an analogue of the more conventional value $n(z)$ (e.g., Zehavi et al. 2005; Kazin et al. 2010). This replacement would not change Eq. (2) and results of following calculations because in that case one should divide both numerator and denominator by the comoving volume (remind that $\sigma(n_c) = \sigma(\mathrm{N}_c)/\mathrm{dV}_c$, where σ is the standard (mean squared) deviation).

[1] http://zmtt.bao.ac.cn/galaxy_clusters
[2] http://www.pha/jhu.edu/ gz323/jhusdss

The power spectrum is calculated for the normalized radial distribution $\mathrm{NN(D}_c\mathrm{)}$ according to the formula (e.g., Jenkins & Watts 1969, Scargle 1982)

$$\mathrm{P}(k_\mathrm{m}) = \frac{1}{\mathcal{N}_\mathrm{b}}\left\{\left[\sum_{j=1}^{\mathcal{N}_\mathrm{b}}\mathrm{NN}_j\cos(k_\mathrm{m}\mathrm{D}_{c,j})\right]^2 + \left[\sum_{j=1}^{\mathcal{N}_\mathrm{b}}\mathrm{NN}_j\sin(k_\mathrm{m}\mathrm{D}_{c,j})\right]^2\right\}, \qquad (3)$$

where $\mathcal{N}_\mathrm{b}$ is a number of bins, $j = 1, 2, ...\mathcal{N}_\mathrm{b}$ is a numeration of bins, $\mathrm{D}_{c,j}$ is a location of bin centers, $k_\mathrm{m} = 2\pi\mathrm{m}/\mathrm{D}_c^\mathrm{L}$ is a wave number, corresponding to an integer harmonic number $\mathrm{m}= 1, 2, ...$, D_c^L is the whole comoving interval. Note that Eq. (3) represents just a square of the discrete Fourier transform, $F_\mathrm{m} = F(k_\mathrm{m})$, responsible for the m-th harmonic (e.g., Groth 1975): $|\mathrm{F_m}|^2 = \mathrm{Re}^2(\mathrm{F_m}) + \mathrm{Im}^2(\mathrm{F_m})$).

We determine also the two-point RCF, $\xi(\delta\mathrm{D}_c)$, for the samples under consideration in an unconventional way (e.g., Papers I and II). The variable $\delta\mathrm{D}_c$ is a radial comoving distance between components of any pair of the objects in the samples. Note that members of different pairs with fixed $\delta\mathrm{D}_c$ may correspond to different mutual comoving distances. Using the estimator by Landy & Szalay (1993) one can introduce

$$\xi(\delta\mathrm{D}_c) = \frac{\mathrm{DD}}{\mathrm{RR}} - 2\frac{\mathrm{DR}}{\mathrm{RR}} + 1, \qquad (4)$$

where $\mathrm{DD} = \mathrm{DD}(\delta\mathrm{D}_c)$ is a number of observed pairs of cosmological objects separated by the radial comoving distance $\delta\mathrm{D}_c$ belonging to a range $\delta\mathrm{D}_c \pm \tilde{\Delta}_c/2$, where $\tilde{\Delta}_c$ is a chosen accumulative bin width; $\mathrm{DR} = \mathrm{DR}(\delta\mathrm{D}_c)$ is a number of cross pairs between points of the real sample and a random sample simulated for the same intervals of D_c and the same smoothed function (trend) as the real one; $\mathrm{RR} = \mathrm{RR}(\delta\mathrm{D}_c)$ is a number of pairs counted up only for the random sample.

We concentrate on the consideration of periodical components incorporated in the radial distributions of the samples relatively to the D_c-variable. We treat these components as *quasi*-periodicities because of limited intervals of line-of-sight distances used for both types of the objects, as well as a dependence of peak positions and amplitudes on sample variations. In Sections 2 and 3 we present the results of statistical analysis of galaxy clusters, traced by the BCGs and absorption systems Mg II, respectively. In Section 4 we confront Fourier transform phases of the main quasi-periodical components with the phase of the dominant quasi-periodical component of the radial distribution of LRGs (Paper III). Conclusions and discussion of the results in a context of the large-scale structure (LSS) of the matter distribution in the Universe are given in Section 5.

2 RADIAL DISTRIBUTIONS OF BRIGHTEST CLUSTER GALAXIES

Fig. 1 demonstrates the radial distribution functions $\mathrm{N(D}_c\mathrm{)}$ calculated for two samples of objects described in Introduction with using independent bins $\Delta_c = 10\ h^{-1}$ Mpc. In both the cases rather narrow spike-like variations of $\mathrm{N(D}_c\mathrm{)}$ stand out against the background of the smoothed trend functions $\mathrm{N}_{\mathrm{tr}}\mathrm{(D}_c\mathrm{)}$ (see Introduction) drawn by the grey curves.

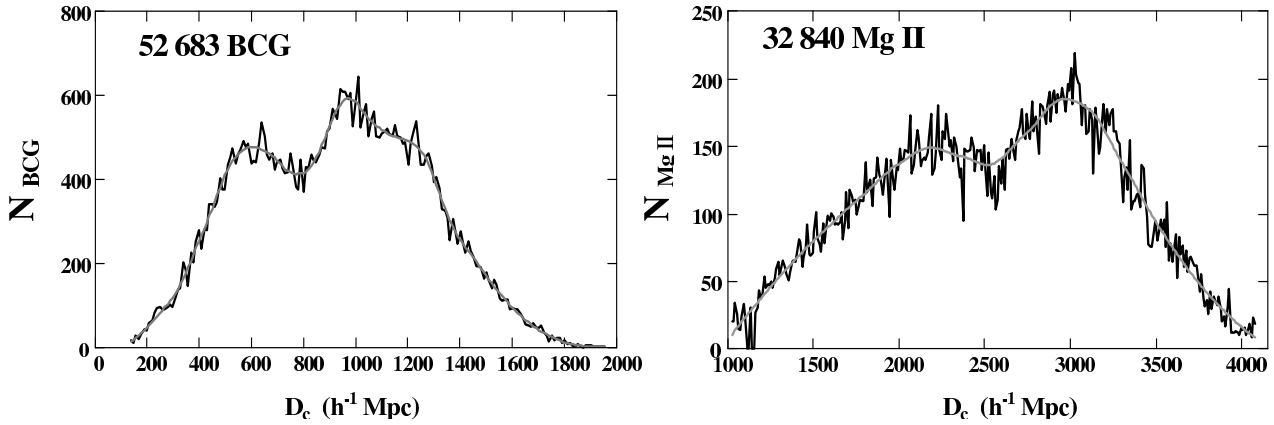

Figure 1. Radial distribution functions $N(D_c)$, where D_c is the line-of-sight comoving distance, calculated in ΛCDM cosmological model with employing of independent bins $\Delta_c = 10$ h^{-1} Mpc for two samples of cosmologically remote objects: *left panel:* 52,683 brightest cluster galaxies (BCGs) within the redshift interval $0.044 \leqslant z \leqslant 0.78$ ($130.8 \leqslant D_c \leqslant 1956.8$ h^{-1} Mpc), *right panel:* 32,840 absorption-line systems Mg II within the redshift interval $0.37 \leqslant z \leqslant 2.28$ ($1018.5 \leqslant D_c \leqslant 4078.5$ h^{-1} Mpc). Grey smoothed curves show the trend functions $N_{tr}(D_c)$.

Employing Eqs. (2) and (3) one can calculate the power spectrum for both the samples. Fig. 2(a) demonstrates the resultant power spectra $P(k)$ of the radial distribution of BCGs. A height of the single significant peak has been slightly increased by a *phase tuning* procedure, i.e., a set of independent shifts of both the boundaries ($D_{c,min}$ and $D_{c,max}$) shortening the interval to reach the visible maximum of the amplitude P_{max} at m=m*. In this way the most significant peak at m=m*=18 or $k = k^* = 0.0644$ h Mpc^{-1} is obtained for the interval $190.8 \leqslant D_c \leqslant 1946.8$ h^{-1} Mpc or $D_c^L = 1756$ h^{-1} Mpc corresponding to the sample of 52,526 BCGs (cf. 52,683 BCGs in Fig. 1). The derived quasi-period is $\Delta D_c = (98 \pm 3)$ h^{-1} Mpc.

To estimate the significance of the main power spectrum peak we use hereafter so-called *false alarm probability* (see Scargle 1982; Frescura, Engelbrecht & Frank 2008 and references therein) treating all spectrum peaks as a result of Gaussian noise:

$$\mathcal{F} = \Pr(P_{max} > \mathcal{P}_0) = 1 - (1 - \exp(-\mathcal{P}_0))^{\mathcal{N}_q}, \qquad (5)$$

i.e., the probability that an amplitude P_{max} of at least one of possible peaks is higher than a value $\mathcal{P}_0$. Here $\mathcal{N}_q$ is the Nyquist number, $\mathcal{N}_q = \mathcal{N}_b/2$, i.e., the maximal number of possible peaks detectable in the power spectrum; in our case $\mathcal{N}_b$ is determined in Eq. (3) as the number of bins. Specifically we have $\mathcal{N}_b = 175$ (BCGs) and $\mathcal{N}_b = 293$ (Mg II). Choosing a given level of the false alarm probability $\mathcal{F} = p_0$ one can confront it with the amplitude $\mathcal{P}_0$ according to the formula $\mathcal{P}_0 = -\ln[1-(1-p_0)^{1/\mathcal{N}_q}]$, or $\mathcal{P}_0 = -\ln[1-\beta^{1/\mathcal{N}_q}]$, where $\beta = 1 - p_0$ is a confidence level. In this paper we use the standard confidence levels $\beta = 0.998$ (3σ), $\beta = 0.999936$ (4σ), and $\beta = 0.9999994$ (5σ) for significance estimations. One can see that the significance of the main peak in Fig. 2(a) slightly exceeds the level 4σ. It evidences in favour of existence of a quasi-periodical component in the radial distribution of BCGs.

Fig. 2(b) represents the power spectrum calculations based on a subsample of the 41,420 most luminous galaxies with absolute magnitudes $M_r \leqslant M_0$ (index "r" stands for SDSS "r"-band) selected from the whole sample of BCGs. The upper limit M_0 was smoothly variated until the main peak amplitude P_{max} in the power spectra reached its maximal value at $M_0 = -23.01$ with the significance exceeding the level 5σ. The power spectra in both left panels are calculated for the same interval of D_c and in the same technique, but the panel (b) represents a reduced number 41,341 BCGs. One can see strong enhancement of the peak amplitude in the panel (b) at the same m=m*=18, $k = k^* = 0.0644$, and $\Delta D_c = (98 \pm 3)$ h^{-1} Mpc as in the panel (a). That increases statistical reliability of the conclusion about occurrence of the quasi-periodical component (signal) in the radial distribution of BCGs. Note, however, that the estimation of the mean value of relative oscillation amplitudes over the whole interval $D_c^L = 1826$ h^{-1} Mpc in this favourable case yields a small number: $< \delta N_{BCG}/N_{tr,BCG} > \sim 0.04$.

The right panels of Fig. 2 display one-dimensional (two-point) normalized RCFs (see Eq.(4)), $\xi(\delta D_c)/\sigma(\xi)$, calculated by counting pairs (across the whole interval $D_c^L = 1826$ h^{-1} Mpc) with fixed radial comoving distance δD_c. To estimate a standard deviation $\sigma(\xi)$ for a set of the values $\xi(\delta D_c)$ we generate 1000 random samples. It is found that the standard deviation can be approximated by $\sigma(\xi) \approx 1/\sqrt{RR}$. In the panels (c) and (d) the curves of grey colour indicate the bounds of the most probable quantities $\xi(\delta D_c)$ restricted by $\pm\sigma$, i.e., the quantities $\xi(\delta D_c)/\sigma(\xi)$ dispersed within a range ± 1. The accumulative bin width is chosen as $\tilde{\Delta}_c = 30$ h^{-1} Mpc and a step of consecutive shifts of this bin is $\delta_c = 1$ h^{-1} Mpc.

Fig. 2(c) shows the normalized RCF of the whole sample 52,683 BCGs. One can see a quasi-periodic behaviour of $\xi(\delta D_c)$. If positions of the peaks (maxima) or depressions (minima) are determined as weighted mean values (centres of gravity, e.g., Paper I) then the mean interval between neighbour peaks (or depressions) matches with the period appeared in the power spectra. Some exception is the first peak located at $\delta D_c \sim 50$ h^{-1} Mpc. Such a peak in power spectra appears for some realizations with minor significance ($\lesssim 3\sigma$) at $k = 0.120$ and $\Delta D_c = 52.3$ h^{-1} Mpc in the course of the *phase tuning* procedure described above. Let us note

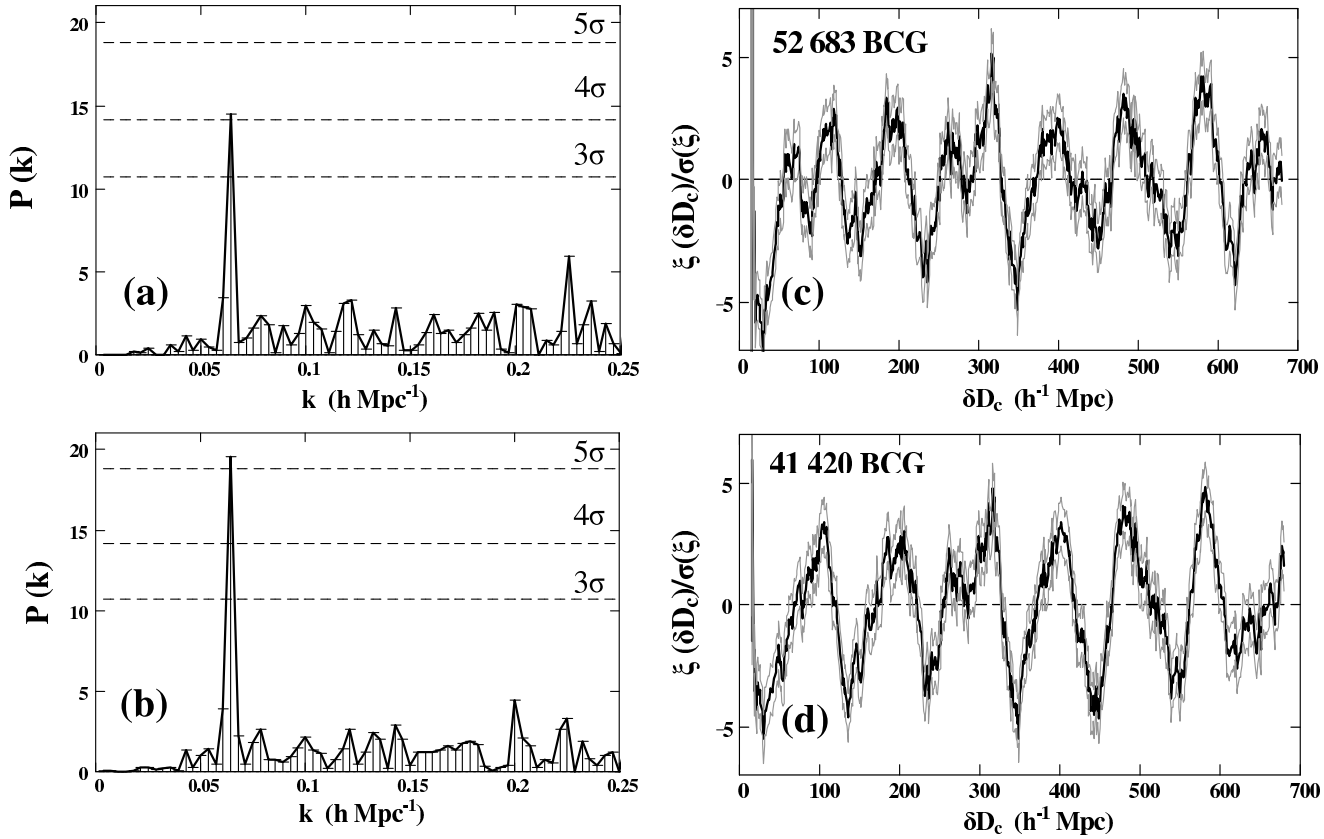

Figure 2. *Left panels* **(a)** and **(b)**: power spectra P(k) with $k = k_{\rm m}$ calculated according to Eq. (3) for two BCG samples in the binning approach with independent bins $\Delta_c = 10$ h^{-1} Mpc within a comoving-distance interval $190.8 \leqslant {\rm D}_c \leqslant 1946.8$ h^{-1} Mpc (cf. Fig. 1) slightly reduced by a phase tuning procedure (see text); the horizontal dash lines specify the significance levels 3σ, 4σ, and 5σ estimated with using Eq. (5) at fixed levels of confidence probability $\beta = 1 - \mathcal{F} = 0.998$, 0.999936, 0.9999994, respectively. Panel **(a)**: P(k) calculated for a slightly reduced number 52,526 of BCGs; panel **(b)**: P(k) calculated for the most luminous 41,341 BCGs at the absolute magnitude $M_{\rm r} \leqslant -23.01$. *Right panels* **(c)** and **(d)**: normalized radial (two-point) correlation function (RCF) (see text) calculated by sliding-average technique with an accumulative bin $\tilde{\Delta}_c = 30$ h^{-1} Mpc and a step of its consecutive shifts $\delta_c = 1$ h^{-1} Mpc in one of two directions from each point of the sample. Grey curves indicate upper and lower boundaries of $\pm\sigma$ band of RCF-values. Panel **(c)**: RCF calculated for the whole sample of 52,683 BCGs shown in the left panel of Fig. 1; panel **(d)**: RCF calculated for the most luminous 41,420 BCGs at $M_{\rm r} \leqslant -23.01$ (see text).

that similar quasi-period was marked also in the radial distributions of the LRGs (see Paper III).

The normalized RCF calculated for a sample of the 41,420 most luminous ($M_{\rm r} \leqslant -23.01$) BCGs is shown in Fig. 2(d). In this case the oscillations of the correlation function is more pronounced. The mean interval between centres of gravity of neighbour peaks (or depressions) is (98.5 ± 2.5) h^{-1} Mpc, that is in a good coordination with the results of spectral analysis. Keeping this in mind we conclude that the most luminous BCGs are the better tracers of the quasi-periodic component in the radial distribution of clusters than the whole sample of BCGs. It seems to be concerned with more noisy statistics of the whole sample.

3 RADIAL DISTRIBUTIONS OF MG II ABSORPTION-LINE SYSTEMS

The right panel in Fig. 1 demonstrates the radial distribution of 32,840 Mg II ALSs within the interval $1018.5\ h^{-1} \leqslant {\rm D}_c \leqslant 4078.5\ h^{-1}$ Mpc ($0.37 \leqslant z_{abs} \leqslant 2.28$) plotted with the same independent bins $\Delta_c = 10\ h^{-1}$ Mpc as it used in the left panel. We consider only so-called intervening absorption systems $z = z_{abs}$ blueshifted from their origin QSOs, z_e, at least by $\Delta z/(1+z_e) \geqslant \Delta v/c$, where $\Delta z = z_e - z_{abs}$, $\Delta v = 14,000$ km/s is the minimal radial-velocity shift allowable for the absorption systems relative to their z_e. Catalog of the Mg II absorption-line doublets cited in Introduction (see also Zhu & Ménard 2013) contains the rest equivalent widths (at $\lambda = 2796\mathring{A}$, first component) distributed in a wide range, $0.02 \leqslant {\rm W}_r(2796) \leqslant 8.4\mathring{A}$.

The left panels in Fig. 3 display the power spectra P(k) plotted for the radial distributions of two Mg II ALS samples in the same way as in Fig. 2. The panel (a) refers to a sample of 32,589 Mg II absorption doublets (cf. 32,840 Mg II ALSs in Fig. 1) and reveals one dominant peak at significance exceeding 4σ. The amplitude of the peak was also increased by the phase tuning procedure (described in Section 2). The confidence probabilities are calculated in the same way as in Fig. 2(a) and (b) at a number of bins $\mathcal{N}_{\rm b} = 293$. In this way the most significant peak at m=29, $k = 0.0622\ h$ Mpc^{-1} is obtained for the interval $1128.5 \leqslant {\rm D}_c \leqslant 4058.5\ h^{-1}$ Mpc, i.e., ${\rm D}_c^{\rm L} = 2930\ h^{-1}$ Mpc. The corresponding quasi-period is $\Delta {\rm D}_c = (101 \pm 2)\ h^{-1}$ Mpc.

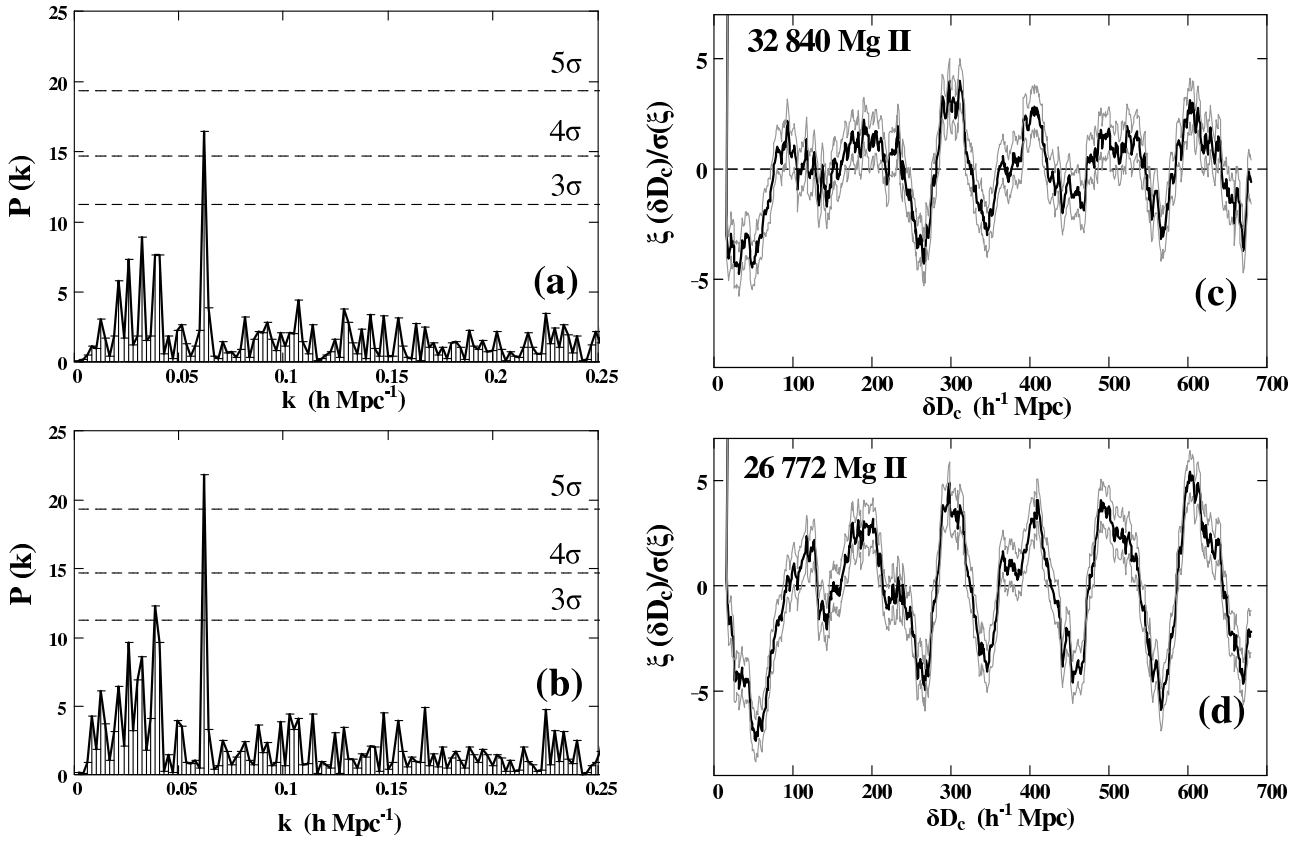

Figure 3. Same as in Fig. 2 but for two samples of Mg II ALSs. *Left panels* **(a)** and **(b)**: power spectra P(k) calculated in the same binning approach (independent bins – $\Delta_c = 10$ h^{-1} Mpc) within a comoving-distance interval $1128.5 \leqslant \mathrm{D}_c \leqslant 4058.5$ h^{-1} Mpc slightly reduced by the phase tuning procedure (see text). The confidence levels (horizontal dashed lines) are also calculated with the use of Eq. (5). Panel **(a)**: P(k) calculated for a slightly reduced number 32,589 of Mg II systems; panel **(b)**: P(k) calculated for a subsample of 26,561 Mg II absorption systems selected with the use of a disjunction of two conditions: $\mathrm{W}_r(2796) < 0.75\AA \bigvee \delta z \leqslant 0.0001$ at $\mathrm{W}_r(2796) \geqslant 0.75\AA$. *Right panels* **(c)** and **(d)**: same as in the panels **(c)** and **(d)** in Fig. 2 but for two Mg II ALSs samples obtained in the same sliding-average approach: the accumulative bin – $\tilde{\Delta}_c = 30$ h^{-1} Mpc and the step – $\delta_c = 1$ h^{-1} Mpc. Panel **(c)**: RCF calculated for the whole sample of 35,840 Mg II absorption systems involved in the distribution represented in the right panel of Fig. 1; panel **(d)**: RCF calculated for a subsample of 26,772 Mg II systems selected with the use of the same conditions as in the panel **(b)**.

Fig. 3(b) represents the power spectrum calculatins based on a subsample of 26,772 Mg II systems submitting to two partly compatible conditions $\mathrm{W}_r(2796) < 0.75\AA$ or $\delta z \leqslant 0.0001$ at $\mathrm{W}_r(2796) \geqslant 0.75\AA$, where δz is an accuracy of the redshifts z_{abs} spectral measuring. These boundaries of the values W_r and δz have been fixed in a process of their smooth variations until the main peak $\mathrm{P}_{\max}$ reached its maximal value with the confidence probability exceeding 5σ. The power spectra in the panels (a) and (b) are also (as in Fig. 2) calculated for the same interval of D_c and in the same technique, but the panel (b) represents a reduced number of 26,561 Mg II systems. Let us emphasize that we get again the strong enhancement of the peak amplitude in the panel (b) at the same m=29, $k = 0.0622$, and $\Delta \mathrm{D}_c = (101 \pm 2)\ h^{-1}$ Mpc. In this case, as in Section 2, the estimation of the mean value of relative oscillation amplitudes over the whole interval $\mathrm{D}_c^{\mathrm{L}} = 3060\ h^{-1}$ Mpc yields a small number $< \delta \mathrm{N}_{\mathrm{MgII}}/\mathrm{N}_{\mathrm{tr,MgII}} > \sim 0.06$.

The right panels in Fig. 3 represent two-point RCF, $\xi(\delta \mathrm{D}_c)/\sigma(\xi)$, calculated by analogy with Fig. 2 for the whole interval $\mathrm{D}_c^{\mathrm{L}} = 3060\ h^{-1}$ Mpc with the same accumulative bin width and the step of consecutive shifts of the bin. In this case we also reproduce 1000 random samples and estimate the standard deviation for a resultant set of RCFs using the same approximation $\sigma(\xi) \approx 1/\sqrt{\mathrm{RR}}$. The grey coloured curves indicate again the bounds of the most probable quantities $\xi(\delta \mathrm{D}_c)/\sigma(\xi)$ restricted by the standard deviations ± 1.

Fig. 3(c) shows a normalized RCF for the whole sample of Mg II doublets. The black and grey curves display a quasi-periodic behaviour of $\xi(\delta \mathrm{D}_c)$. The mean interval between centres of gravity of neighbour peaks (or depressions) turns out to be consistent with the period corresponding to the main peak of the power spectra.

Fig. 3(d) demonstrates the normalized RCF calculated for the sample of 26,772 Mg II ALSs satisfying the same two conditions as used in Fig. 3(b). Similar to Fig. 2 one can see an increase of the oscillation amplitudes. The mean interval between centres of gravity of neighbour peaks proves to be $(101 \pm 2)\ h^{-1}$ Mpc, that is also in good coordination with the results of the spectral analysis.

4 PHASES OF QUASI-PERIODICAL COMPONENTS

Results represented in Sections 2 and 3 are compatible with existence of the most significant quasi-periodical component at a characteristic scale $(101 \pm 6)\ h^{-1}$ Mpc in the radial distribution of LRGs (Paper III) mentioned in Introduction. Fig. 4 demonstrates a comparison of phases of the Fourier transformations produced for the LRGs from one side and for BCGs and Mg II ALSs from the other. In both panels of Fig. 4 the same thick solid line represents a sum of five harmonics calculated as the reciprocal Fourier transformation of the radial distribution of LRGs at $5 \leqslant \mathrm{m} \leqslant 9$.

Specifically, for the radial distribution of the LRGs we use an approximate expression:

$$\mathrm{NN(D}_c) \approx \frac{2}{\sqrt{\mathcal{N}_\mathrm{b}}} \sum_{\mathrm{m_{min}}}^{\mathrm{m_{max}}} |\mathrm{F_m}(k_\mathrm{m})| \cos(k_\mathrm{m}\mathrm{D}_c - \varphi_\mathrm{m}), \qquad (6)$$

where $\mathrm{F_m}(k_\mathrm{m})$ is the discrete Fourier amplitude introduced in the comments to Eq. (3), $|\mathrm{F_m}| = \sqrt{\mathrm{P}(k_\mathrm{m})}$, $k_\mathrm{m} = 2\pi\mathrm{m}/\mathrm{D}_c^\mathrm{L}$ is a wave number and $\varphi_\mathrm{m} = \arctan(\mathrm{Im\,F_m}/\mathrm{Re\,F_m})$ is a phase of m-th harmonic; in our case $\mathrm{m_{min}} = 5$ and $\mathrm{m_{max}} = 9$. Note that the main contribution to the curve is provided by two harmonics: m=6, $(135 \pm 12)\ h^{-1}$ Mpc and the dominant at m=8, $(101 \pm 6)\ h^{-1}$ Mpc.

One can see that the mutual phase relations in the left and right panels of Fig.4 are different. In the left panel the thick curve is compared with a thin line or the single spatial oscillation at m=18 corresponding to the peak in the power spectrum obtained for the most luminous 41,341 BCGs (Fig. 2b). In the right panel the thick curve is confronted with the single spatial oscillation at m=29 (thin line) corresponding to the peak in the power spectrum obtained for the 26,561 Mg II ALSs (Fig. 3b). Both the spatial oscillations are calculated with the use of Eq. (6) at the fixed m.

In the left panel the phases of the main quasi-periodical components of the LRGs and BCGs are close. Thus LRGs and galaxy clusters (or BCGs) trace the same elements of the large-scale structure (LSS) of cosmologically remote objects. It is not surprisingly because, as it was emphasized by Wen & Han (2013), majority of SDSS galaxy clusters includes LRGs as member galaxies or the brightest galaxies inside clusters. Note, however, that the statistics of BCSs does not completely coincide with that of LGRs.

In the right panel the phases of the main quasi-periodical components calculated for the LRGs and Mg II systems turn out to be approximately opposite: mutually shifted at a phase angle $\sim \pi$. If these results were confirmed it would mean that the LRG and Mg II ALS samples trace, as a rule, different elements of the LSS. For instance, if LRGs indicate regions with enhanced densities of dark matter then Mg II systems concentrate in regions with reduced densities. This assumption gets a qualitative support in a visual pattern of the combined LRGs and Mg II absorbers spatial distributions represented by SubbaRao et al. (2008). Although, the problem of spatial correlations of Mg II absorbers is considered to be rather complicated (e.g., Lundgren et al. 2009; Matejek & Simcoe 2012).

5 CONCLUSIONS AND DISCUSSION

The main results of the statistical treatment of 52,683 brightest cluster galaxies (BCGs) from the SDSS DR9 within the redshift interval $0.044 \leqslant z \leqslant 0.78$ (Wen & Han 2013) and 32,840 Mg II absorption-line systems (ALSs) from SDSS DR7 within the interval $0.37 \leqslant z \leqslant 2.28$ (Zhu & Ménard 2013) can be summarized as follows:

(1) The radial (line-of-sight) 1D-distribution of BCGs incorporates a significant quasi-periodical component with respect to the smoother radial selection function (trend). The dominant peak in the power spectra demonstrates the periodicity corresponding to a spatial characteristic scale $\Delta\mathrm{D}_c = (98 \pm 3)\ h^{-1}$ Mpc at a level of significance $\gtrsim 4\sigma$. Still more prominent spectral peak, $\gtrsim 5\sigma$, corresponding to the same scale is obtained in the power spectrum calculated for a subsample of the 41,420 most luminous BCGs with absolute magnitudes $M_\mathrm{r} \leqslant -23.01$. Let us emphasize, however, that the mean value of relative amplitudes of the oscillations averaged over the whole interval D_c^L for the latter subsample turns out to be small ~ 0.04.

(2) The existence of the quasi-periodicity in the radial distribution of BCGs has been confirmed also by the two-point radial (1D) correlation function $\xi(\delta\mathrm{D}_c)$ displaying the periodicity in the explicit form.

(3) The radial distribution of Mg II ALSs also includes a significant quasi-periodical component with respect to the trend. The dominant peak in the power spectra corresponds to a scale $\Delta\mathrm{D}_c = (101 \pm 2)\ h^{-1}$ Mpc at the same significance level $\gtrsim 4\sigma$ as for the BCGs. We also obtain an enhancement of the peak height for the radial distribution of 26,772 Mg II systems separated out by two partly compatible conditions: $\mathrm{W}_r(2796) < 0.75\mathring{A}$ or $\delta z \leqslant 0.0001$ at $\mathrm{W}_r(2796) \geqslant 0.75\mathring{A}$, where δz is an accuracy of redshift z_{abs} detections. In the latter case the mean value of relative amplitudes of the oscillations averaged over the whole interval D_c^L is also small ~ 0.06. Note that similar scale $\sim 100\ h^{-1}$ Mpc of the C IV ALSs correlation function within a range $1.2 < z < 4.5$ was found also by Quashnock, Vanden Berk & York (1996).

(4) The two-point radial (1D) correlation function $\xi(\delta\mathrm{D}_c)$ also visualizes the quasi-periodical component in the radial distribution of Mg II ALSs corresponding to the same scale as the peak in the power spectra.

(5) Both the quasi-periodical scales found here in the radial distributions of two different types of cosmological objects are consistent with the quasi-periodicity scale $(101 \pm 6)\ h^{-1}$ Mpc found earlier (Paper III) in the radial distribution of the luminous red galaxies (LRGs). The phases of the main periodical components, calculated as reciprocal Fourier transforms, turn out to be approximately close for the BCGs and LRGs and approximately opposite (shifted at a phase angle $\sim \pi$) for the Mg II ALSs and LRGs.

(6) All considered quasi-periodical scales (partly overlapping) are consistent with the scale $(102.2 \pm 2.8)\ h^{-1}$ Mpc of the baryon acoustic peak in the two-point spatial (3D-monopole) correlation function of the LRGs (Blake et al. 2011). It is likely that there are implicit relations between the quasi-periodicities found here in the radial distributions of cosmological objects and the characteristic scale of sound horizon, r_s, at the recombination epoch (so called *standard ruler*; e.g., Blake & Glazebrook 2003; Percival et al. 2007;

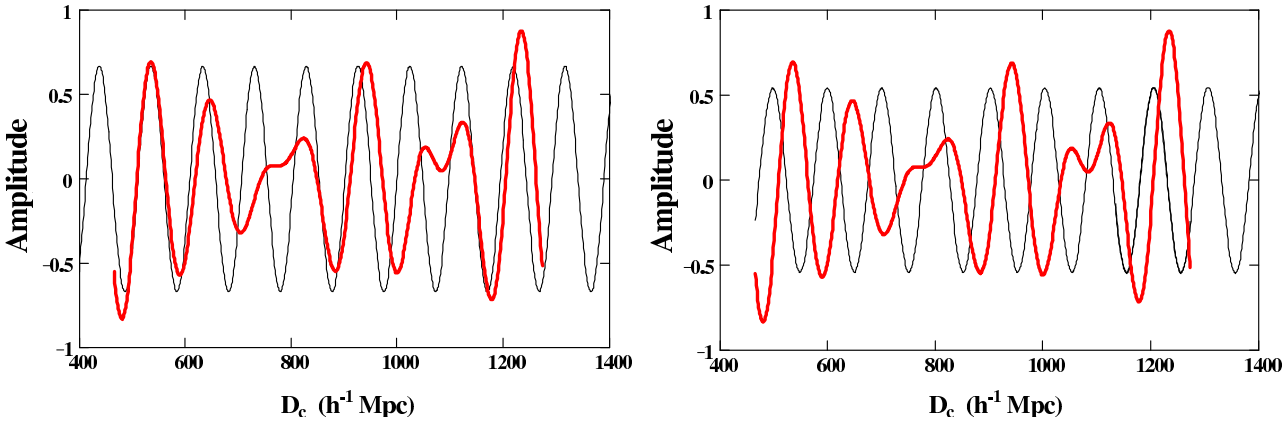

Figure 4. (Colour online) Reciprocal Fourier transformation produced for five harmonics $5 \leqslant m \leqslant 9$ calculated in Paper III for the radial distribution of 105,831 LRGs (thick solid lines) versus two reciprocal Fourier components (thin lines) calculated in the present work. *Left panel*: harmonic number m=18, ($\Delta D_c = (98 \pm 3)$ h^{-1} Mpc) corresponding to the single significant peaks in Figs. 2**(a)** and **(b)**. *Right panel*: harmonic number m=29 ($\Delta D_c = (101 \pm 2)$ h^{-1} Mpc) corresponding to the single significant peak in Figs. 3 **(a)** and **(b)**.

Eisenstein et al. 2007; Percival et al. 2010; Anderson et al. 2012). In that case further confirmation and specification of the quasi-periodicity in radial distributions would become a simple and alternative tool for an express-analysis of vast arrays of cosmological data. On the other hand, the proximity of the scales of the baryon acoustic peak and those treated in the present paper may evidence in favour of an assumption that primordial acoustic perturbations responsible for the BAO-scale could carry traces of a partly ordering formed at some early epochs, e.g., recombination or radiation-matter equipartition.

For instance, one can imagine a weak tendency of galaxies to be distributed as a continuous structure of higher and lower densities (a set of cells) formed by standing acoustic waves (e.g., Zeldovich & Novikov 1983, Hu, Sugiyama & Silk 1997, Eisenstein et al. 2007) with dominant characteristic scale $\sim r_s$. This structure may display itself in some apparent arrangement of the matter distribution, as a consequence of a possible relatively dense packing of the cells. In such a context the hypothesis of a weak (linear) partial ordering of matter imprinted in the epoch of recombination (at $z \lesssim z_{rec} \sim 10^3$) may relate to a conception of a quasi-regular network formed by voids and galaxy superclusters at the nonlinear stage ($z \ll z_{rec}$), which was discussed, e.g., in a series of papers by Einasto et al. (e.g., Einasto et al. 1997a,b,c; Einasto 2000; Tago et al. 2002; Einasto et al. 2011).

An illustration of the ordering possibilities was represented also in Paper II. There was simulated a model of partly ordered structure of points (galaxies or galaxy clusters) forming a cloud-like scattering around the vertices of a simple cubic (SC) lattice. For this model it was produced a mean power spectrum averaged over 100 random realizations of the radial distribution function. The mean spectrum displays a significant peak at $k = 2\pi/l_{SC}$, where l_{SC} is a lattice constant and resembles the spectrum shown in Fig. 2(a). That reflects a general property of the radial distribution of the lattice points with an arbitrary centre of the space. In this case the resultant radial distribution exhibits a periodical behaviour with a constant amplitude of oscillations (e.g., Kendall & Moran 1963).

To elucidate the relation between the oscillations observable in 3D-power spectrum, displaying the BAO phenomenon, and quasi-periodical component in the radial distribution, revealed in this work, we carried out some additional simulations. To be specific, we produced a square matrix of complex Fourier amplitudes $F(k_x, k_y)$ in a 2-dimensional k-space, where k_x and k_y are two projections of the wave vector $\mathbf{k}$, $k^2 = k_x^2 + k_y^2$, and $\mathrm{Re}(F(k_x, k_y))$ and $\mathrm{Im}(F(k_x, k_y))$ obey the Gaussian distributions, which are modulated by harmonic variations with smoothly decreasing (damped) amplitudes. The damping is similar to the observable baryon oscillations in 3D-k-space (e.g., Eisenstein & Hu 1998; Blake & Glazebrook 2003; Anderson et al. 2012). Then we transformed the generated in such a way square matrix of $F(k_x, k_y)$ into the distribution of points in the real 2D-space and applied the analysis described in Introduction to random realizations of the distribution obtained.

Our preliminary results have shown that at some decreasing dependences of the amplitudes at $k = k_1, k_2, k_3...$, where $k_1, k_2 = 2k_1, k_3 = 3k_1...$ – positions of the oscillation maxima, the power spectrum Eq. (3) of the radial distribution displayed a set of descending narrow peaks at the same $k = k_1, k_2, k_3....$ Note that subsequent peaks cab be less significant than the first ones. Moreover, the radial distribution turns out to be sensitive to harmonic loops of a 2D-k-distribution transforming them to narrower peaks in the related 1D-k-space, i.e., intensifying one (or a few) discrete radial harmonic(s). On the other hand, in the real 2D-space we obtain only one noticeable peak of the standard (multicentral) correlation function. That reminds the well-known peak of the 3D-correlation function (e.g., Eisenstein et al. 2005; Kazin et al. 2010; Blake et al. 2011; Ross et al. 2012) specific for the BAO phenomenon in the real space. Being confirmed these results could reconcile the baryon oscillations in the k-space with quasi-periodicities of the radial distribution in the real space.

It is likely as well that the quasi-periodicities formu-

lated in items (1)-(5) concern with the well known results by Broadhurst et al. (1990) widened and confirmed by Szalay et al. (1993). Their pencil-beam surveys near both the Galactic poles within a redshift interval $z \lesssim 0.5$ displayed a periodicity at a scale 128 h^{-1} Mpc. Quasi-periodicities in two-dimensional patterns obtained on the base of the Las Campanas Redshift Survey data had been also found by Landy et al. (1996) as a power-spectrum peak corresponding to a scale of $\sim 100\ h^{-1}$ Mpc in the spatial distribution of galaxies. This scale is rather close to the scales found here in the radial distributions of the BCGs and Mg II ALSs, and found earlier for the LRGs. Possible relations of the cited periodicities with the spatial scale of BAOs $\sim 100\ h^{-1}$ Mpc were discussed by Eisenstein et al. (1998) and Szalay (1998). Szalay et al. (1993) emphasized the special role of rich-statistics pencil-beam surveys in bringing out the phase correlations (regularities) of matter density fluctuations. They expected systematic decrease and broadening of the power spectrum peaks for wider angle regions of observational samples.

Note, however, that the region of the SDSS DR9 survey on the sky (e.g., Ahn et al. 2012) includes only the north galactic pole. Additional elimination from the sample of all objects within solid angles at $\theta \leqslant 5^\circ$ around the pole axis does not effect noticeably the radial quasi-periodical component of the rest sample of BCGs. Thus the effect of total radial distribution considered here in a sense differs from the effects discussed by Broadhurst et al. (1990) and Szalay et al. (1993). Although, it is likely that there is some implicit relation between these two approaches which still have to be manifested in a future.

In reality quasi-periodical components of the matter distribution may appear as a consequence of two (or a few) factors, e.g., effects of clumping of galaxies and their clusters (e.g., Kaiser & Peacock 1991) and/or quasi-ordering of the matter spatial distribution (discussed above). It is likely that the modern surveys of the sky deal with a complex mixture of both (or more) the factors. In any case, the quasi-periodicity revealed here being confirmed probably traces some spatial partly-ordered structure imprinted in the LSS of matter in the early Universe.

Acknowledgments The work has been supported partly by the Research Program OFN-17, Division of Phys., RAS and by the State Program "Leading Scientific Schools of Russian Federation" (grant NSh-294.2014.2).

References

Abazajian K. N., et al., 2009. ApJS, 182, 543
Ahn C. P., et al., 2012, ApJS, 203, 21
Anderson L. et al, 2012, MNRAS, 427, 3435
Bassett B. A., Hlozek R., 2009, preprint (arXiv:0910.5224)
Blake C., Glazebrook K., 2003, ApJ, 594, 665
Blake C. et al., 2011, MNRAS, 418, 1707
Broadhurst T. J., Ellis R. S., Koo D. C., Szalay A. S., 1990, Nature, 343, 726
Einasto J., 2000, preprint (arXiv:astro-ph/0011334)
Einasto J. et al., 1997a, Nature, 385, 139
Einasto J. et al., 1997b, MNRAS, 289, 801
Einasto J., Einasto M., Frisch P., Gottlöber S., Müller V., Saar V., Starobinsky A. A., Tucker D., 1997c, MNRAS, 289, 813
Einasto J. et al., 2011, A&A, 531, A75
Eisenstein D. J., Hu W., 1998, ApJ, 496, 605
Eisenstein D. J., Hu W., Tegmark M., 1998, ApJ, 504, L57
Eisenstein D. J., Hu W., Silk J., Szalay A.S., 1998, ApJ, 494, L1
Eisenstein D. J. et al., 2005, ApJ, 633, 560
Eisenstein D. J., Seo H-J., White M., 2007, ApJ, 664, 660
Frescura F. A. M., Engelbrecht C. A., Frank B. S., 2008, MNRAS, 388, 1693
Groth E. J., 1975, ApJS, v.29, No. 286, 285
Hogg D. W., 1999, preprint (astro-ph/9905116)
Hu W., Sugiyama N., Silk J., 1997, Nature, 386, 37
Jenkins G. M., Watts D. G., 1969, Spectral analysis and its applications, Holden-Day
Kaiser N., Peacock J. A., 1991, ApJ, 379, 482
Kazin E. A. et al., 2010, ApJ, 710, 1444
Kayser R., Helbig P., Schramm T., 1997, A&A, 318, 680
Kendall M. G., Moran P. A. P. 1963, Geometrical Probability, New York: Hafner
Landy S. D., Szalay A. S., 1993, ApJ, 412, 64
Landy S. D., Shectman S. A., Lin H., Kirshner R. P., Oemler A. A., Tucker D., 1996, ApJ, 456, L1
Lundgren B. F. et al., 2009, ApJ, 698, 812
Matejek M. S., Simcoe R. A., 2012, ApJ, 761, 112
Percival W. J., Cole S., Eisenstein D. J., Nichol R. C., Peacock J. A., Pope A. C., Szalay A. S., 2007, MNRAS, 381, 1053
Percival W. J. et al., 2010, MNRAS, 401, 2148
Quashnock J. M., Vanden Berk D. E., York D.G., 1996, ApJ, 472, L69
Ross A. J. et al., 2012, MNRAS, 424, 564
Ryabinkov A. I., Kaminker A. D., Varshalovich D. A., 2007, MNRAS, 376, 1838 (Paper I)
Ryabinkov A. I., Kaminker A. D., 2011, ApSS, 331, 79 (Paper II)
Ryabinkov A. I., Kaurov A. A., Kaminker A. D., 2013, ApSS, 344, 219 (Paper III)
SubbaRao M. U., Aragón-Calvo M. A., Chen H. W., Quashnock J. M., Szalay A.S., York D.G., 2008, New Journal of Physics, 10, 125015
Scargle J. D., 1982, ApJ, 263, 835
Szalay A. S., 1998, in Olinto A. V., Frieman J. A., Schramm D. N., Edge R. N. J., 8-th Texas Symposium on Relativistic Astrophysics and Cosmology, World Scientific, p. 136
Szalay A. S., Broadhurst T. J., Ellman N., Koo D. C., Ellis R. S., 1993, Proc. Natl. Acad. Sci. USA, Vol. 90, 4853
Tago E., Saar E., Einasto J., Einasto M., Müller V., Andernach H., 2002, AJ, 123, 37
Wen Z. L., Han J. L., 2013, in Thomas D., Pasquali A., Ferreras I., eds, Proc. IAU Symp. No. 295, The intriguing life of massive galaxies; preprint [arXiv: 1301.0871]
Zehavi I. et al., 2005, ApJ, 621, 22
Zeldovich Y.B., Novikov I.D., 1983, Relativistic Astrophysics, V2: The Structure and Evolution of the Universe, University of Chicago Press, Chicago
Zhu G., Ménard B., 2013, ApJ, 770, 130